

Hyperspectral 3D Reconstruction for Non-destructive Plant Nutrient Analysis

Gerry Chen, Yongsheng Chen, Cédric Pradalier

Abstract—Resource use efficiency in agriculture is becoming increasingly important as the world population grows and climate change impacts food production. Accordingly, precision agriculture adoption is growing, but requires more accurate plant growth modeling and monitoring to be most effective. The plant phenotyping community has devised many techniques for non-destructively estimating plant properties such as mass, stress state, and nutrient concentration using computer vision and specialized sensors. In particular, computer vision techniques have been used to analyze plant structure while hyperspectral data has been used to analyze plant nutrient concentrations at a field- or plant- level. We seek to combine these techniques to measure the nutrient *distribution* within a plant over time to better model how nutrient flows dictate plant growth. In this preliminary work, we collect a dataset of 6 sets of ~50 images towards constructing hyperspectral 3D reconstructions of plants.

I. INTRODUCTION

As environmental conservation is becoming an increasingly important issue, efficient agricultural practices which maximize output while minimizing resource input and environmental impact are imperative to exercise and further develop. For example, according to the EPA, nitrogen fertilizer alone contributes, in the form of N₂O, at least 4.1% of total US greenhouse gas emissions [1]. Meanwhile, current farming practices encourage excess, blanket applications of fertilizer as opposed to the targeted, “smart” applications as part of the growing precision agriculture movement being made possible by recent advances in sensors, data, and AI [2].

Plant growth models are imperative for precision agriculture to predict crop yields under various conditions. In controls terms, we must model the system dynamics of the biological plant to apply optimal control. Therefore, farmers seek real-time, actionable data on their crops while researchers seek more, better data to study growth models. Plant biomass, nutrient content, and other properties are of particular interest to both farmers and researchers.

Existing methods for analyzing plant mass and nutrient content are destructive: they require harvesting the plant to weight it, dehydrate it, and send it to a lab for testing. This is not only expensive, but also significantly limits the quantity and statistical significance of data collected. For example, studying plant growth often requires tracking plant metrics as it grows, but destructive analyses make it impossible to measure the same plant multiple times since the first measurement requires killing the plant. Instead, many sets of plants must be grown under identical conditions and periodically harvested for analysis.

Robotics and computer vision may offer significant value by enabling non-destructive methods for analyzing plant proper-

ties. Prior works have shown how 3D reconstructions from RGB imagery can be effectively used to estimate plant mass and growth, while other works have shown how hyperspectral (HS) imagery can be used to estimate nutrient content, health, photosynthetic efficiency, and growth regions of plants. However, only limited works have studied 3D HS reconstructions. Prior works have projected HS data onto 3D reconstructed surfaces or generated 3D surfaces using HS reconstructions directly, but none consider HS data in volumetric representations, which may offer insight into the 3D structural/spatial distribution of plant properties and more accurate whole-plant nutrient content estimations.

II. RELATED WORK

In this review, Section II-A summarizes how hyperspectral (HS) imaging is used in plant monitoring and analysis, Section II-B discusses 3D reconstruction especially as applied to plants, and Section II-C discusses works that attempt to create 3D reconstructions in the HS color space.

A. Hyperspectral Imaging

HS imaging is becoming an increasingly useful tool in plant analysis since it can be used to track the concentrations of different resources, nutrients, and molecules across the plant. Since different molecules reflect light differently in different wavelengths, scientists have been able to correlate different spectral reflectances with concentrations of certain molecules such as common forms of macro- and micro-nutrients, water, and chlorophyll. While the total space of works studying is vast, [3]–[6] are reviews of the most common applications and techniques for HS imaging in plant analysis.

HS super-resolution is a research area that aims to reduce the challenges associated with collecting HS imagery by predicting HS imagery from less intensive sensors. In addition to the cost and portability challenges associated with HS cameras, HS cameras tend to have a tradeoff between spatial, temporal, and wavelength resolution. HS-from-RGB is a standardized task [7] with benchmarks and datasets that aim to predict HS imagery from RGB imagery, but is not currently sufficiently accurate for the small signals required for plant analysis. In the future, fine-tuning on large amounts of plant-specific imagery may improve the suitability of HS-from-RGB for plant analysis. Other HS super-resolution tasks to predict HS data from multi-spectral (MS) imagery or improve the spatial resolution of HS images (e.g. by fusing the high spatial resolution of HS imagery with the high wavelength resolution of MS imagery) [8], [9]. Although HS super-resolution is an interesting and related field, we plan to use an off-the-shelf

HS camera to limit the scope of our work. Future works may see direct estimation of nutrient and other distributions within plants by using HS super-resolution techniques and intermediate HS ground-truth supervision.

B. 3D Reconstruction

This section has been significantly abbreviated since modern off-the-shelf RGB SfM and photogrammetry softwares are of very high quality. For additional background, please refer to [10].

1) Sensors: Almost all 3D reconstruction methods (even those that also use additional sensors) leverage RGB cameras given their ubiquity, low cost, and richness of information afforded by the high resolution. I will discuss works using RGB-only, direct-depth, and structured-light.

RGB-only methods, thanks to advances in structure-from-motion and multi-view stereo that have produced high quality off-the-shelf photogrammetry packages, have become sufficiently accurate for many applications. [10]–[13] use a single high-resolution SLR camera to manually take photographs and use photogrammetry methods to create full 3D reconstructions. The reconstructions can be computed and analyzed for leaf geometry analysis in 20–30 minutes. [14] applies a very similar method but using a handheld stereo camera rig rather than monocular. [15] also uses stereo cameras, but also investigates leveraging salient outer-contour features in addition to traditional (sparse) 3D reconstructions. [16], [17] both focus on estimating large-scale crop field biomass (not focusing on single-plant measurements), with [16] using UAV imagery and [17] using fixed monitoring stations with cameras.

Discussion of other sensor types, such as IR-based depth, ToF-based depth, light-field cameras, and structured-light based systems are omitted for brevity, but are common in plant phenotyping literature.

2) NeRF: Neural Radiance Fields (NeRF) is a recent development in the multi-view stereo step of structure-from-motion which uses deep learning to learn a model describing the spatial radiance properties of the object [18]. In the standard formulation, an MLP is used to represent the 4D RGB+radiance as a function of 5D camera position and view-angle. By representing not only the surface point-cloud (as with e.g. SfM) but instead a volumetric representation, we believe NeRF techniques will be particularly useful for HS imaging since plant structures are not opaque in all wavelengths.

3) Applications: 3D reconstruction of plants is most often used to track plant growth. Plant growth can be tracked through total plant biomass estimates [10], [13], [15]–[17], [19] or through individual plant organ segmentation [12], [20], [21]. As compared to 2D approaches to plant phenotyping (e.g. top-down image only), 3D methods are able to provide more comprehensive and accurate data about plant growth. Therefore, we believe that reasoning about HS data in 3D will allow us to better analyze plant growth from a nutrient use+transport+accumulation perspective.

C. Hyperspectral 3D Reconstruction

HS 3D reconstruction is an understudied area, with only 6 papers to the authors' knowledge addressing it directly. In [22]–[25], RGB-only data is used to create 3D pointclouds, onto which 2D HS images are projected. This does not allow insight as to the HS radiance densities inside the plant. In [26], [27], separate (grayscale) 3D pointclouds are made using each HS band then fused together. Since different organs have different reflectance properties in different wavelengths, many wavelengths may have incomplete or failed reconstructions which limits the accuracy of this late-fusion approach. In [28], a HS structured-light capturing system is created which enables direct generation of a HS point-cloud, but this approach is highly customized.

It is our belief that a HS 3D reconstruction approach using NeRF techniques can produce more complete HS reconstructions including of internal structures, which will enable more detailed modeling of plant nutrient uptake, transport, and accumulation. [8] is the closest work to our proposed approach, which uses an MLP implicit representation to perform 2D HS super-resolution, but does not extend to 3D, possibly due to the lack of a suitable dataset and benchmark.

III. APPROACH

In this work, we will perform hyperspectral 3D reconstruction, that is: 3D reconstruction using hyperspectral images to obtain point clouds where each point specifies the intensities of ~ 128 wavelengths. We will collect preliminary data, qualitatively assess the data from pseudo-RGB images, and validate that the images are of sufficient quality by generating 3D reconstructions from the pseudo-RGB images. In the future, we will implement baseline approaches for full 3D hyperspectral reconstruction and implement our proposed NeRF-based solution.

A. Preliminary Data Collection

We seek to collect a preliminary dataset consisting of 50 hyperspectral images from various viewpoints for each of 3 plants of varying species. The images will be taken using the SOC 710-VP hyperspectral camera from Surface Optics. Due to the long exposure time (23s-3min), we are limited to this small preliminary dataset. Additionally, we will use a manually positioned tripod to take the images to ensure that the camera remains stable for the duration of each exposure. The 50 images will be taken as 2 full “rings” (roughly 30° per yaw update) at different elevations (elevations will vary depending on plant species). For each ring, the camera will remain stationary and the plant will rotate on a servo-controlled turn-table to provide partial ground-truth information for the camera poses. 4 different plants (of different species) will be used for 6 image sets to capture a variety of plant structures and nutrient concentrations.

Figure 1 depicts the imaging setup.



Fig. 1. The imaging setup with SOC710-VP hyperspectral camera (on the right of each image) and the turntable visible as the black circular platform supporting the each plant. The two images show the two camera elevations used for the “rings”. The top image shows a lettuce plant and the bottom image a basil plant.

B. Pseudo-RGB

We produce pseudo-RGB images by taking the appropriate wavelengths from the hyperspectral data to use as the red, green, and blue channels respectively. Although we could in principle use a weighted average based on common camera filter spectra, we find that using a single wavelength channel for each of the R, G, and B channels produces sufficiently informative images. We choose to use 620nm, 555nm, and 503nm for red, green, and blue respectively.

C. Pseudo-RGB 3D Reconstruction

We validate the quality of the images by creating 3D reconstructions from the pseudo-RGB data. Under the assumption that the selected wavelengths for the R, G, and B channels are representative of the other wavelengths in the hyperspectral data, successfully generating 3D reconstructions from the pseudo-RGB data would indicate that the hyperspectral data is of sufficient quality to generate full 3D reconstructions including all the wavelengths. We use the open-source, off-the-shelf COLMAP [29], [30] Structure-from-Motion package.

D. Preliminary Baseline Data Analysis (Future Work)

To establish the quality of existing hyperspectral 3D reconstruction methods, we will implement the approaches from [23] and [27]. The results will be compared qualitatively and quantitatively. We will seek to compare the hyperspectral responses of the points in the point cloud to the known reflectances of different nutrients and to the known nutrient

concentrations of different organs of the plants. Because existing hyperspectral nutrient estimation approaches often require extensive calibration against a reference dataset of plants from the same species, inter-species comparisons may be less meaningful than comparisons amongst different plant organs of the same plants. The significance of hyperspectral 3D reconstruction over traditional hyperspectral nutrient estimation may be supported by inter-organ comparisons.

E. Preliminary NeRF Data Analysis (Future Work)

I hypothesize that:

- 1) NeRF will enable us to achieve more accurate hyperspectral point clouds specifically for the wavelength bands that are transparent or translucent in plants.
- 2) NeRF will enable us to estimate the inner structure of a plant, since certain plant organs are typically translucent in certain wavelengths, and NeRF is capable of reasoning about translucency thanks to its differentiable rendering in training.

To test this hypothesis, we will implement and test hyperspectral NeRF on the 3 preliminary datasets. We will compare the comprehensiveness of the reconstructions as compared to the baselines (in all the wavelengths), compare the noise-levels of all the reconstructions, and qualitatively inspect the reconstructions to see if NeRF is able to reconstruct the inner structure of the plants.

IV. RESULTS & DISCUSSION

In this section, we present the hyperspectral dataset we collected, pseudo-RGB images from the dataset, and 3D reconstructions using pseudo-RGB images from HS data.

A. Hyperspectral Data

Overall, we qualitatively observe that the images collected by the hyperspectral camera are of good quality and appear to be sufficient for 3D reconstructions. They appear to be of sufficient resolution to make out structural details in the plants. They also have minimal distortion and relatively low noise. However, images at longer wavelengths are slightly out-of-focus. Additionally, the exposure time of each image was very long (2.5 minutes/image) (see Section V-D for more details).

An example hyperspectral image is visualized in Figure 2. Each hyperspectral image in the dataset contains 128 wavelengths at 696x520 resolution, making it a 128x696x520 tensor which is commonly referred to as a hyperspectral “cube” in the hyperspectral camera industry.

We can observe in Figure 2 that the lower wavelength images are sharper than the higher wavelength images. Despite best efforts to calibrate the focus of the camera during data collection, it was not possible to achieve perfect focus for all wavelengths. This is further discussed in V-C.

To compensate for the emission spectrum of the light source (which is meant to imitate “sunlight”), we can use a standard color calibration board (Figure 3) or compare the brightness of the plants against the background, which can be assumed to be gray. Limitations are discussed in Section V-A.

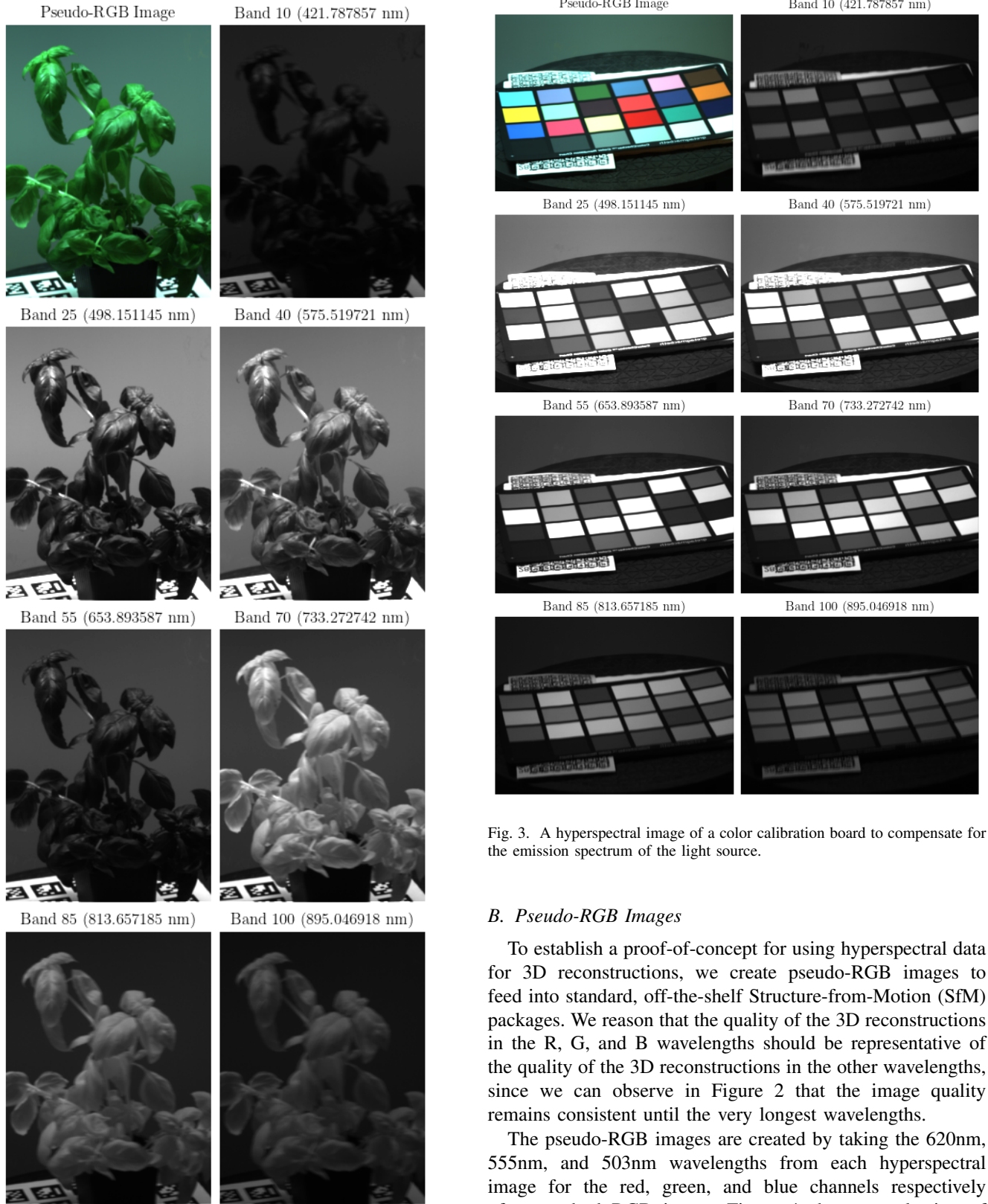


Fig. 2. A depiction of a hyperspectral “cube” making up a single hyperspectral image in our dataset. A subset of 7 of the 128 wavelengths are shown, as well as a pseudo-RGB image generated by taking the 620nm, 555nm, and 503nm wavelengths for the red, green, and blue channels respectively.

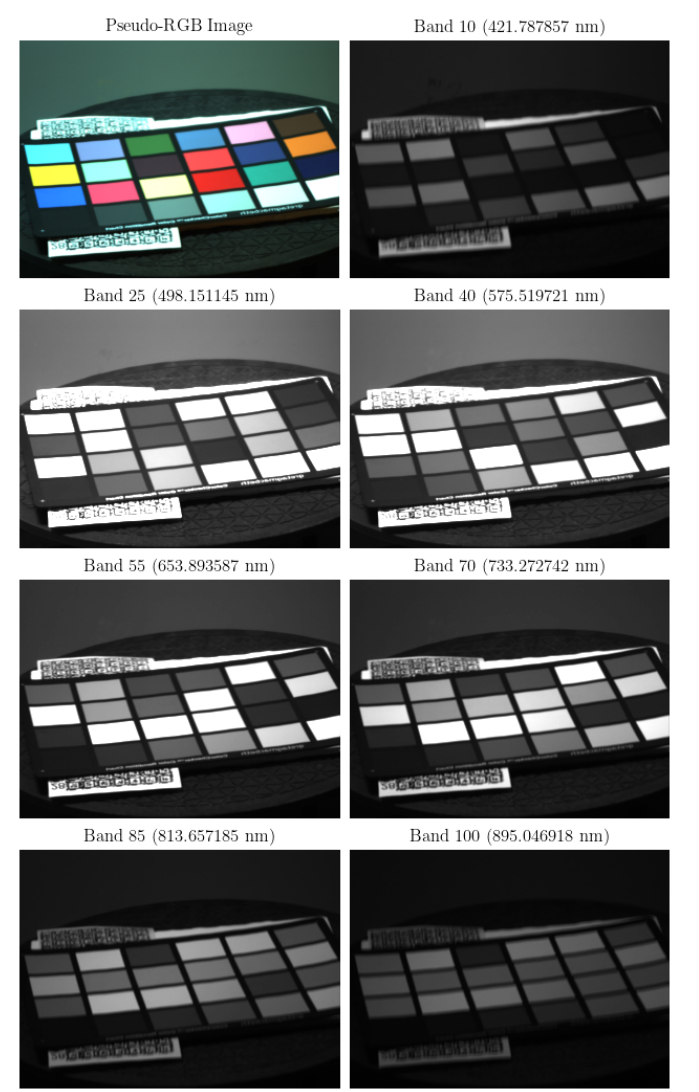


Fig. 3. A hyperspectral image of a color calibration board to compensate for the emission spectrum of the light source.

B. Pseudo-RGB Images

To establish a proof-of-concept for using hyperspectral data for 3D reconstructions, we create pseudo-RGB images to feed into standard, off-the-shelf Structure-from-Motion (SfM) packages. We reason that the quality of the 3D reconstructions in the R, G, and B wavelengths should be representative of the quality of the 3D reconstructions in the other wavelengths, since we can observe in Figure 2 that the image quality remains consistent until the very longest wavelengths.

The pseudo-RGB images are created by taking the 620nm, 555nm, and 503nm wavelengths from each hyperspectral image for the red, green, and blue channels respectively of a standard RGB image. Figure 4 shows a selection of pseudo-RGB images from our dataset and conveys the camera viewpoints imaged for each plant.

One observation that can be made (easier to recognize in video form than in image-mosaic form) is that the lettuce and

basil plants noticeably wilted throughout the duration of data collection (2 hours/plant). This can be partially attributed to the laboratory environment and inability to carefully control soil moisture, but is also a fundamental limitation of the long image exposure time (2.5 minutes/image, see Section V-D).

C. 3D Reconstructions

The 50 RGB images for each plant are fed into COLMAP [29], [30]: an off-the-shelf open-source SfM package. Two example resulting 3D reconstructions are shown in Figure 5. Some background outlier points were manually removed, but could be automatically removed in the future using a similar algorithm as the one in [10]. Qualitatively, the outliers were easy to identify based on their physical separation from the rest of the points in the point cloud (e.g. use DBSCAN) and based on their color: a large proportion of outliers were not green in color.

The 3D reconstruction quality is very good and suggests that the reconstruction quality using the full hyperspectral data should be good as well. The camera poses, which are required for NeRF, are also expected to have low error given the high quality of the reconstructions. Quantitative verification based on the fact that the turntable gives us partial ground truth data (relative pose/orientation is fixed for each ring, except for one rotational angle which changes by exactly 15°/image) can also be done in the future.

One observation is that the topmost leaves of the basil plant (Figure 5 right) appear to be less well reconstructed than the rest of the plant. This is suspected to be due to the plant wilting throughout the course of the data collection, especially these leaves, violating the assumption that the plant subject is static across the images.

V. LIMITATIONS & FUTURE WORKS

There are several limitations that we have discovered in the course of this work, some due to our methodology and others due to fundamental limitations of current hyperspectral camera technology.

A. Light Source Spectrum Calibration

The standard Pantone color calibration board used for color calibration is only intended for RGB calibration and does not guarantee particular reflectances in the full hyperspectral sensor range. Our dataset contains calibration images of a standard Pantone color calibration board and of an 11"x8.5" AprilCal calibration board [31].

One standard method of calibrating the light source spectrum is to use a spectrometer to measure the light source spectrum and then use that spectrum to generate a light source spectrum image. However, the camera itself may not be perfectly calibrated so its readings may differ slightly from the spectrometer's.

Another standard method is to use a standard "gray" reflectance cube which reflects a known percentage of light evenly across a certified range of wavelengths. This has the added benefit of compensating for any camera sensor mis-calibrations.

B. Non-Lambertian Reflectance

A phenomenon related to light spectrum calibration is that of non-Lambertian reflectance, whereby the reflectance of a surface is not constant across all angles. This is a common phenomenon in plants, where the reflectance of a leaf may be different depending on the angle of the light source. This is a fundamental limitation of hyperspectral imaging, and is not specific to our work, but must nonetheless be considered when attempting to use hyperspectral imaging for nutrient estimation and structural analysis.

Several methods in the computer vision literature have been proposed to address this issue, including in NeRF in which the color and opacity of a point in space is a function of not only the point's position but also the view direction ray (camera view angle).

C. Wavelength-dependent Focus

This is due to an effect similar to chromatic aberration, whereby the dependence of refractive index on wavelength causes a lens to focus different wavelengths of light differently. Therefore, it is impossible to keep all wavelengths of light in focus simultaneously. This has been confirmed by the camera manufacturer to be a fundamental limitation of the technology.

One approach is to use a smaller aperture, which has the effect of increasing the depth-of-field and thereby decreasing the amount any part of the image is out-of-focus. Unfortunately, this also increases the exposure time and/or decreases the SNR, which is already long to begin with (see V-D).

Another approach is to find better material lenses or use focusing mirrors, but these tend to have more restrictive fields-of-view. The SOC710-VP camera we use in this work already has one of the widest fields of view of any camera on the market and has a field-of-view of just 11.4°, requiring the camera to be more than a meter away to capture a full plant. For the automated imaging robot described in [10], this is unacceptably narrow as is, and traditional optics with less chromatic aberration would likely only exacerbate this issue.

Finally, the last approach is to use lower-level sensor mechanisms. The SOC710-VP camera and many similar field-oriented hyperspectral cameras have internal mechanical mechanisms to capture images through a "pushbroom" mechanism that captures one-line of the image at a time. We could instead use lower-level mechanisms and scan ourselves to alleviate lensing and field-of-view issues, but this would require a custom-built camera and would be prohibitively time consuming.

D. Exposure Time

The long exposure time causes challenges in throughput and accuracy. Throughput is obviously reduced because imaging a single plant takes prohibitively long as it currently stands, even for a robotic imaging system. At 2 hours per plant, only 12 plants could be imaged in a 24 hour period which is too small a sample size to be scientifically useful. In terms of accuracy, plants change appreciably over the course of hours every day, due to growth and circadian cycles. The assumption



Fig. 4. A selection of pseudo-RGB images of basil (left) and rosemary (right) from our dataset are shown to illustrate the different view angles imaged for each plant. For each plant, the left and right columns display images from the 2 different “rings” (elevations) described in Section III-A. Pseudo-RGB images are generated by taking the 620nm, 555nm, and 503nm wavelengths for the red, green, and blue channels respectively.



Fig. 5. Visualizations of the 3D reconstructions of rosemary (left) and basil (right) plants from pseudo-RGB data.

that the plant is static across images appears to still be mostly reasonable in our dataset, but certainly becomes less valid for more leafy plants (e.g. lettuce) and is somewhat visible in Figure 5, where the top-most leaves of the basil plant (which visibly moved due to wilting) appear to be less well constructed than the rest of the plant.

The exposure time of the camera is long, requiring 2min14sec per image. This is due to the tradeoff between spatial, spectral, and “temporal” resolution of hyperspectral cameras. With a fixed imaging sensor size, the imaging sensor must be exposed longer to receive enough photons to produce a large enough SNR. This is especially challenging for the higher wavelengths due to the IR noise from the camera’s internal components (e.g. black body radiation). As compared to RGB cameras, hyperspectral cameras need many more sensor pixels to sense more wavelengths. With a fixed sensor size, scene, and optics, it is not currently possible to simultaneously have high image resolution (spatial), many wavelength bands (spectral), and short exposure time (temporal).

One approach is to increase the aperture size to let in more light, but we already established in V-C that this is problematic due to chromatic aberration.

Another approach is to illuminate the scene with stronger lights. This is certainly possible to a point, but too much light can burn the plants or affect the scientific experiment by providing the plants with more light than controlled-for. Under strong daylight conditions, the exposure time should theoretically be able to be reduced to around 30seconds, which may or may not be achievable in our controlled experimental testbed. Even 30 seconds is still long, requiring around half-an-hour per plant, and applying full-daylight conditions may cause more plant movement during imaging.

VI. CONCLUSIONS

In this work, we collected a preliminary dataset of hyperspectral images and performed 3D reconstruction, towards creating full hyperspectral 3D reconstructions to better model how nutrient distribution and flow affect plant growth.

We found several challenges associated with hyperspectral imaging technology, including long exposure time, chromatic aberration, and narrow field-of-view. However, we found that the quality of the images, once captured, were sufficient to generate 3D reconstructions from pseudo-RGB images.

We anticipate that we will be able to successfully generate full hyperspectral 3D reconstructions using this preliminary dataset, and that we will be able to see structural differences in reflectance spectra between different plant organs and species. Finally, we anticipate that a future full dataset, containing a larger sample size and ground-truth nutrient concentrations, would enable us to estimate nutrient concentrations in plants more comprehensively than existing hyperspectral approaches.

REFERENCES

- [1] EPA, “Draft inventory of u.s. greenhouse gas emissions and sinks: 1990–2020, chapter 5: Agriculture,” U.S. Environmental Protection Agency, Tech. Rep. EPA 430-R-22-003, 2022.

- [2] A. R. Cohen, G. Chen, E. M. Berger, S. Warrier, G. Lan, E. Grubert, F. Dellaert, and Y. Chen, "Dynamically controlled environment agriculture: Integrating machine learning and mechanistic and physiological models for sustainable food cultivation," *ACS ES&T Engineering*, vol. 2, no. 1, pp. 3–19, 2022. [Online]. Available: <https://doi.org/10.1021/acsestengg.1c00269>
- [3] R. Sarić, V. D. Nguyen, T. Burge, O. Berkowitz, M. Trtílek, J. Whelan, M. G. Lewsey, and E. Čustović, "Applications of hyperspectral imaging in plant phenotyping," *Trends in Plant Science*, vol. 27, no. 3, pp. 301–315, 2022. [Online]. Available: <https://www.sciencedirect.com/science/article/pii/S1360138521003460>
- [4] L. Li, Q. Zhang, and D. Huang, "A review of imaging techniques for plant phenotyping," *Sensors (Basel)*, vol. 14, no. 11, pp. 20078–20111, Oct 2014.
- [5] P. Pandey, Y. Ge, V. Stoerger, and J. C. Schnable, "High throughput in vivo analysis of plant leaf chemical properties using hyperspectral imaging," *Frontiers in Plant Science*, vol. 8, 2017. [Online]. Available: <https://www.frontiersin.org/articles/10.3389/fpls.2017.01348>
- [6] M. Wahabzada, A.-K. Mahlein, C. Bauckhage, U. Steiner, E.-C. Oerke, and K. Kersting, "Plant phenotyping using probabilistic topic models: Uncovering the hyperspectral language of plants," *Scientific Reports*, vol. 6, no. 1, p. 22482, 2016. [Online]. Available: <https://doi.org/10.1038/srep22482>
- [7] B. Arad, O. Ben-Shahar, R. Timofte, L. Van Gool, L. Zhang, M.-H. Yang, Z. Xiong, C. Chen, Z. Shi, D. Liu, F. Wu, C. Lanaras, S. Galliani, K. Schindler, T. Stiebel, S. Koppers, P. Seltsam, R. Zhou, M. El Helou, F. Lahoud, M. Shahpaski, K. Zheng, L. Gao, B. Zhang, X. Cui, H. Yu, Y. B. Can, A. Alvarez-Gila, J. van de Weijer, E. Garrote, A. Galdran, M. Sharma, S. Koundinya, A. Upadhyay, R. Manekar, R. Mukhopadhyay, H. Sharma, S. Chaudhury, K. Nagasubramanian, S. Ghosal, A. K. Singh, A. Singh, B. Ganapathysubramanian, and S. Sarkar, "Ntire 2018 challenge on spectral reconstruction from rgb images," in *2018 IEEE/CVF Conference on Computer Vision and Pattern Recognition Workshops (CVPRW)*, 2018, pp. 1042–104209.
- [8] K. Zhang, "Implicit neural representation learning for hyperspectral image super-resolution," 2021. [Online]. Available: <https://arxiv.org/abs/2112.10541>
- [9] X.-H. Han, Y. Zheng, and Y.-W. Chen, "Hyperspectral image reconstruction using multi-scale fusion learning," *ACM Trans. Multimedia Comput. Commun. Appl.*, vol. 18, no. 1, jan 2022. [Online]. Available: <https://doi.org/10.1145/3477396>
- [10] G. Chen, H. Muriki, C. Pradalier, Y. Chen, and F. Dellaert, "A hybrid cable-driven robot for non-destructive leafy plant monitoring and mass estimation using structure from motion," 2022. [Online]. Available: <https://arxiv.org/abs/2209.08690>
- [11] A. Paproki, X. Sirault, S. Berry, R. Furbank, and J. Fripp, "A novel mesh processing based technique for 3d plant analysis," *BMC Plant Biology*, vol. 12, 2012.
- [12] J. Christian Rose, S. Paulus, and H. Kuhlmann, "Accuracy analysis of a multi-view stereo approach for phenotyping of tomato plants at the organ level," *Sensors (Switzerland)*, vol. 15, no. 5, pp. 9651–9665, 2015.
- [13] J. Walter, J. Edwards, G. McDonald, and H. Kuchel, "Photogrammetry for the estimation of wheat biomass and harvest index," *Field Crops Research*, vol. 216, pp. 165–174, 2018.
- [14] Z. Ni, T. F. Burks, and W. S. Lee, "3d reconstruction of plant/tree canopy using monocular and binocular vision," *Journal of Imaging*, vol. 2, no. 4, 2016. [Online]. Available: <https://www.mdpi.com/2313-433X/2/4/28>
- [15] R. N. Lati, S. Filin, and H. Eizenberg, "Plant growth parameter estimation from sparse 3d reconstruction based on highly-textured feature points," *Precision Agriculture*, vol. 14, no. 6, pp. 586–605, 2013.
- [16] J. Bendig, A. Bolten, S. Bennertz, J. Broscheit, S. Eichfuss, and G. Bareth, "Estimating biomass of barley using crop surface models (csms) derived from uav-based rgb imaging," *Remote Sensing*, vol. 6, no. 11, pp. 10395–10412, 2014.
- [17] S. Brocks and G. Bareth, "Estimating barley biomass with crop surface models from oblique rgb imagery," *Remote Sensing*, vol. 10, no. 2, 2018.
- [18] F. Dellaert, "NeRF explosion 2020," <https://dellaert.github.io/NeRF/>, December 16.
- [19] D. Andújar, C. Fernández-Quintanilla, and J. Dorado, "Matching the best viewing angle in depth cameras for biomass estimation based on poplar seedling geometry," *Sensors (Switzerland)*, vol. 15, no. 6, pp. 12999–13011, 2015.
- [20] G. Azzari, M. L. Goulden, and R. B. Rusu, "Rapid characterization of vegetation structure with a microsoft kinect sensor," *Sensors (Switzerland)*, vol. 13, no. 2, pp. 2384–2398, 2013.
- [21] G. Alenyà, B. Dellen, and C. Torras, "3d modelling of leaves from color and tof data for robotized plant measuring," in *Proceedings - IEEE International Conference on Robotics and Automation*, 2011, pp. 3408–3414.
- [22] N. Brusco, S. Capeletto, M. Fedel, A. Paviotti, L. Poletto, G. M. Cortelazzo, and G. Tonello, "A system for 3d modeling frescoed historical buildings with multispectral texture information," *Machine Vision and Applications*, vol. 17, no. 6, pp. 373–393, 2006. [Online]. Available: <https://doi.org/10.1007/s00138-006-0026-2>
- [23] M. H. Kim, T. A. Harvey, D. S. Kittle, H. Rushmeier, J. Dorsey, R. O. Prum, and D. J. Brady, "3d imaging spectroscopy for measuring hyperspectral patterns on solid objects," *ACM Trans. Graph.*, vol. 31, no. 4, jul 2012. [Online]. Available: <https://doi.org/10.1145/2185520.2185534>
- [24] J. I. Nieto, S. T. Monteiro, and D. Viejo, "3d geological modelling using laser and hyperspectral data," in *2010 IEEE International Geoscience and Remote Sensing Symposium*, 2010, pp. 4568–4571.
- [25] Y. Manabe, S. Kurosaka, and K. Chihara, "Simultaneous measurement of spectral distribution and shape," in *Proceedings 15th International Conference on Pattern Recognition. ICPR-2000*, vol. 3, 2000, pp. 803–806 vol.3.
- [26] A. Zia, J. Liang, J. Zhou, and Y. Gao, "3d reconstruction from hyperspectral images," in *2015 IEEE Winter Conference on Applications of Computer Vision*, 2015, pp. 318–325.
- [27] T. Ma, Y. Xing, D. Gong, Z. Lin, Y. Li, J. Jiang, and S. He, "A deep learning-based hyperspectral keypoint representation method and its application for 3d reconstruction," *IEEE Access*, vol. 10, pp. 85266–85277, 2022.
- [28] Y. Xu, A. Giljum, and K. F. Kelly, "A hyperspectral projector for simultaneous 3d spatial and hyperspectral imaging via structured illumination," *Opt. Express*, vol. 28, no. 20, pp. 29740–29755, Sep 2020. [Online]. Available: <https://opg.optica.org/oe/abstract.cfm?URI=oe-28-20-29740>
- [29] J. L. Schönberger and J.-M. Frahm, "Structure-from-motion revisited," in *Conference on Computer Vision and Pattern Recognition (CVPR)*, 2016.
- [30] J. L. Schönberger, E. Zheng, M. Pollefeys, and J.-M. Frahm, "Pixel-wise view selection for unstructured multi-view stereo," in *European Conference on Computer Vision (ECCV)*, 2016.
- [31] A. Richardson, J. Strom, and E. Olson, "AprilCal: Assisted and repeatable camera calibration," in *Proceedings of the IEEE/RSJ International Conference on Intelligent Robots and Systems (IROS)*, November 2013.